Asian Journal of Scientific Research

ISSN 1992-1454

science alert
http://www.scialert.net

ANSInet
an open access publisher
http://ansinet.com

Asian Journal of Scientific Research 4 (3): 236-245, 2011
ISSN 1992-1454 / DOI: 10.3923/ajsr.2011.236.245

Study of the Wind Tunnel Effect on the Drag Coefficient (C_D) of a Scaled Static Vehicle Model Compared to a Full Scale Computational Fluid Dynamic Model

Sanwar A. Sunny
Department of Mechanical Engineering, School of Engineering, The University of Kansas, Lawrence KS 66045, USA

ABSTRACT

The current study highlighted the relationship between the drag coefficients (C_D) of two models of varying scales but sharing geometric and dynamic similitude. Applying principles of fluid mechanics, especially Bernoulli's law and by scaling models using Reynold's Number (Re) and the Buckingham Pi Theorem at varying velocities u_0, drag forces F_D were found by conducting wind tunnel tests. The scaled drag coefficient was then compared to a full scaled model in a virtual wind tunnel setting of a Computational Fluid Dynamic (CFD) program. Discrepancies were addressed and error margins were discussed. Real analysis (C_D of 0.4) show a 10% deviation from the literature data (C_D of 0.44) while a thorough computational test (C_D of 0.428) showed 2.73% reduction from real manufacture data, contributed to the negligence of the governing flow equations of Navier Stokes, such as modeling principles relative to turbulence. In all, virtual simulation maintained a 7% increase from real test data which is attributed wholly to boundary conditions at the start of computational tests. CFD shortcomings, mainly from exclusion of turbulence during computation are discussed by briefly introducing and comparing Reynolds-Averaged Navier Stokes Equations (RANS) and the Large Eddy Simulation (LES) Techniques.

Key words: Coefficient of drag, Computational fluid dynamics (CFD), similitude, wind tunnel, turbulence

INTRODUCTION

Simple wind tunnels use elementary principles of fluid mechanics to study lift and drag forces on a solid body. A beam balance or strain gauge typically measures changes in elongation at the base of the body in a static setting. In most real analysis of drag forces, however, certain error is bound to occur for a complex body. This is especially true in the case of vehicles. Force fluctuations occur during the rotation of wheels when it is in direct contact with the road surface. Although these differences are usually neglected in simplified experiments, they are crucial in understanding the behavior of a complex body. Computation Fluid Dynamics (CFD) software can successfully create a virtual setting with real parameters and considerations, thereby eliminating some errors to a degree (Zheng *et al.*, 2001). Reynold's number (Re) is an important parameter for CFD testing of flow characteristics for drags and lift behavior in simple forms such as cylinders (Shirani, 2001) to complex designs of automobiles and airplanes (Zhang *et al.*, 2007). Furthermore, Strouhal number is also observed in computational simulation (Ul Islam and Zhou, 2009). Various softwares such as FLUENT and COSMOS Floworks can successfully conduct computational tests and generate virtual fluid flow over a solid body. This ability enables cars and planes to be modeled and tested accordingly (Wang *et al.*, 2005). Other software includes PHOENICS where 3-D models

in CAD use computational airflow to monitor fluid behavior around the car body (Chen *et al.*, 2004). Recent developments in drag reduction include environmental friendly agents that smoothen the surface that the fluid travels on (Abdul Bari *et al.*, 2011). The present study will highlight both elementary and complex principles underlying the behavior of automotive drag coefficient and correctly computing the value in both real and virtual settings.

For years, the aerospace and automotive industries have been enhancing designs to lower the overall drag coefficient by streamlining the exterior panels and choosing different materials. Minimizing losses to drag and other external frictional forces, gives the vehicle more power to reach its optimal peak. In other words, reducing certain parameters optimizes the overall vehicle fuel efficiency. The drag coefficient which is a directly proportional constant to drag forces can be reduced by minimizing the frontal area of a body and deflecting airflow away from sudden, sharp or hollow contours. Turbulence also plays an important part in computational studies and necessary steps have to be taken to correctly model the system and solve complicated turbulence models and equations, mainly Navier-Stokes equations to account for errors within calculations (Liu, 2006).

In this study, the real and virtual behavior of drag forces will be highlighted, culminating in the measurement of the drag coefficient of a certain vehicle, the 1970s VW Super Beetle. Comparing results from both procedures, the reasons for inconsistencies can be observed and external design improvements can be made. Principles of Similitude shall be applied to scale the actual full sized car down to a 1:10 scale model. Due to similarity in overall form, Reynolds Number (Re) will give the scaling factor for the effective velocities. Drag coefficient is the same for two bodies of exact shape but different sizes. In other words, scaling does not affect a model's coefficient of drag as long as the model and the full scale object are of the same exact shape. Pixelizations can be used to quantify the respective vehicles' frontal areas. This data will be supplemented and compared to literature data provided by Volkswagen and also measured using Computer Aided Design (CAD) 3 Dimensional drawings of the actual vehicle. Applications and recommendations will also be discussed.

MATERIALS AND METHODS

A resin material is mixed under guided conditions and hardened at room temperature after letting it cure for 3 h. Epoxy or polyepoxide, a thermosetting polymer is formed from the reaction of an epoxide "resin" with polyamine "hardener". As such, this epoxy is called the two part resin (the resin being a powder and the hardener being a liquid). This material will be applied to the model to provide a desired consistency and is very similar to the smoothness of convention sheet metal or fiber glass which the vehicle exterior is made out of. Vacuum forming was initially used to produce a shell of the vehicle on which the material was poured. Finally, the model is secured to the wind chamber of a wind tunnel by a metal bracket.

An industrial fan provides air that travels over the static body. In principle, this effect is the equivalent of the body moving through the air. The air pushes on the body while traveling around the tested object causing drag forces from above and lift forces from below. The air flow then travels into a pipe and pushes fluids up the venture meter tube and fluctuates the fluid height (measured as Δh). The elongation readings, caused by the flow of air on the body are sent to the control panel of a data acquisition software through a transducer. From these readings, corresponding drag forces are measured. Figure 1 shows the setup of equipment.

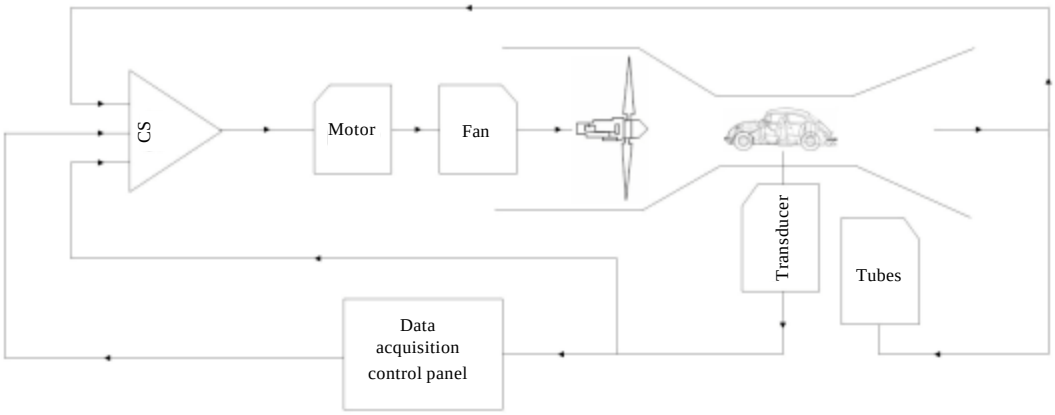

Fig. 1: Wind Tunnel Experimental Setup

Mathematical analysis: Drag forces (F_D) of a car are depended on C_D, the coefficient of drag for the certain shape, ρ_{air}, the mass density of the fluid through which the body is traveling, $A_{frontal}$ or the vehicle's effective frontal area and most importantly u, the mean velocity of the car. $A_{frontal}$ is calculated both manually through photo pixelization and computationally through taking a section view and measuring the enclosed area in a 3-D CAD software. The value of $A_{frontal}$ was 0.0221 m^2.

Using the algorithms of the Pi Theorem, the drag forces which depend on the five above parameters; or f_x (F_D, u, $A_{frontal}$, ρ_{air}, v_0) can be reduced using two dimensionless parameters culminating in the Reynolds number (Buckingham 1914).

Where drag coefficient can be characterized as:

$$F_D = f_z\left(\frac{u\sqrt{A}}{\nu}\right)\cdot\left(\frac{1}{2}\rho_{air}A_{frontal}u^2\right)$$

and then:

$$\frac{1}{2}f_z(Re)\rho_{air}A_{frontal}u^2$$

Where:

$$C_D = \left(\frac{2}{\rho_{air}A_{frontal}}\right)\left(\frac{F_D}{v_0^{\,2}}\right)$$

assuming f_z (Re) = C_D which finally yields:

$$F_D = \frac{1}{2}C_D\rho_{air}A_{frontal}u^2 \quad (1)$$

To scale the velocities for the car and the model, we use principles of geometric similitude by comparing the Reynolds's number, knowing:

$$Re = \frac{u\sqrt{A}}{v}$$

where, $v = \mu/\rho$ (v is the fluid viscosity, ρ is the fluid density and μ is the kinematic viscosity) and we assume $\sqrt{A} = D$ (in meters), hence the number now becomes:

$$Re = \frac{\rho u D}{\mu}$$

and we can establish the relationship between the model and the full scale car by the respective Reynolds numbers. Hence:

$$\left[\frac{\rho u D}{\mu}\right]_{scaled} = \left[\frac{\rho u D}{\mu}\right]_{full}$$

where, the vehicle velocity ratio is given by:

$$u_{scaled} = u_{full} \times \left(\frac{\rho_{full}}{\rho_{scaled}}\right) \times \left(\frac{D_{full}}{D_{scaled}}\right) \times \left(\frac{\mu_{scaled}}{\mu_{full}}\right)$$

the densities ρ and kinematic viscosities μ cancel out due to the fluids being the same (air under standard temperature and pressure) or $u_{scaled} = 10 \times u_{full}$; meaning that for the scaled model to experience the same magnitude of drag forces as a full scaled vehicle, the wind speeds in which it needs to run in would need to be 10 times the wind speed needed for the actual car. This speed would be noted on the venture meter height readings or H (cm) and the changes in height (Δh) will correspond to changes in velocities u (mph). There exists a direct method of establishing a relationship between height readings and wind tunnel air speeds. It is now known universally as the Bernoulli's Principle (Bernoulli *et al.*, 2004).

The work-energy theorem can be used to derive Bernoulli's principle (Tipler, 1991). $W = \Delta E_k$ i.e., the change in the kinetic energy E_k of the system is equal to the net work W done on the system; the system itself consists of a volume of incompressible fluid, between two distinct cross sectional areas given by A_1 and A_2 moving over the distances d_1 and d_2, respectively where $d_i = v_i \Delta t$. The displaced fluid volumes are A_1d_1 and A_2d_2; implying that the displaced masses are ρA_1d_1 and ρA_2d_2, hence $\rho A_1d_1 = \rho A_1v_1\Delta t = \Delta m$ and $\rho A_2d_2 = \rho A_2v_2\Delta t = \Delta m$ (with ρ being the fluid's mass density, Δt being the time interval through which the masses are displaced and the displaced mass denoted by Δm). The work done by pressure along the areas.

$W_p = F_{p,1}\, d_1 - F_{p,2}\, d_2$ which equals $p_1A_1d_1 - p_2A_2d_2$ which become:

$$\Delta m\frac{p_1}{\rho} - \Delta m\frac{p_2}{\rho}$$

the work done mostly by gravity (the gravitational potential energy in the volume A_1d_1 is lost and at the outflow in the volume A_2d_2 is gained) can be written as $\Delta W_g = \Delta mgz_2 - \Delta mgz_1$ according to Feynman *et al.* (1963). And so, $W_g = -\Delta E_g = \Delta mgz_1 - \Delta mgz_2$ the total work done in this time interval Δt being $W_t = W_g + W_p$ which means an increase in kinetic energy given by:

$$\Delta E_k = \frac{1}{2}\Delta m u_2^2 - \frac{1}{2}\Delta m u_1^2$$

hence putting all these together, the work-kinetic energy theorem can be rearranged into the following term:

$$\Delta m\frac{p_1}{\rho} - \Delta m\frac{p_2}{\rho} + \Delta m g z_1 - \Delta m g z_2 = \frac{1}{2}\Delta m u_2^2 - \frac{1}{2}\Delta m u_1^2$$

or:

$$\frac{1}{2}\Delta m u_1^2 + \Delta m g z_1 + \Delta m\frac{p_1}{\rho} = \frac{1}{2}\Delta m u_2^2 + \Delta m g z_2 + \Delta m\frac{p_2}{\rho}$$

and simplify it (diving by the mass, Δm) to:

$$\frac{1}{2}u_1^2 + g z_1 + \frac{p_1}{\rho} = \frac{1}{2}v_2^2 + g z_2 + \frac{p_2}{\rho}$$

giving us:

$$\frac{1}{2}u^2 + g z + \frac{p}{\rho} = K$$

where, K is a constant. It is then multiplied by the fluid density (ρ) throughout the equation gives us:

$$\frac{1}{2}\rho u^2 + \rho g z + p = K$$

or $q+\rho gh = p_0+\rho gz = K$ (Oertel *et al*., 2004) where the dynamic pressure head is given by:

$$q = \frac{1}{2}\rho u^2$$

the hydraulic head by:

$$h = z + \frac{p}{\rho g}$$

and the total pressure is denoted by $p_0 = p+q$. Therefore, normalization of the constant in the equation gives:

$$H=z+\frac{p}{\rho g}+\frac{u^2}{2g}$$

(H being the total energy head) meaning:

$$h+\frac{u^2}{2g}$$

and assuming H-h = Δh, velocity is simply given by $u=\sqrt{2g\Delta h}$ or more specifically, taking into account the fact that the fluid is air, velocity is:

$$u=\sqrt{\frac{2SG\rho g\Delta h}{\rho_{air}}} \quad (2)$$

RESULTS AND DISCUSSION

During the operational time period of 12 minutes, the following data were collected manually (venture meter tube heights and using the Eq. 2, the mean velocities) and automatically (Strain gauge data through transducer on the Labview software as Matlab data points converted to Drag Forces in Newton). The experiment flow chart of the system is shown in Fig. 1:

Increasing Drag Coefficient (iC_D) is 0.39 and Decreasing Drag Coefficient (dC_D) is 0.41 With Full Scale Output (FSO) being 0.40 or 6.6% error within the tests according to Hysteresis Error:

$$\%error_{hyst}=\left(\frac{(iC_D-dC_D)}{FSO}\right)\times 100$$

The actual drag coefficient of this model of the Volkswagen is 0.44 (Aird, 2000), much higher than the results furnished by the wind tunnel (0.40 with a 10% error margin with the literature data). The wind tunnel provided data for fluid height elevation and strain gauge elongation, denoting wind velocity (u) and drag forces (F_D), respectively (Table 1). The gap in the data Table 1 shows hysteresis error observation which was around 6.6%. Equations 1 and 2 were numerically solved with the given data to find the Coefficient of Drag. An increased C_D means that it is harder for the fluid to flow over the body. This difficulty can be contributed to the full scale car due to air flow causing disturbances underneath the car and at the wheels. The tested scaled model did not have wheels attached to it, nor was it resting on the ground. Moreover, external parts were taken off, such as side view mirrors and exhaust piping, all of which add restrictions for the flow of air past the body. The value of 0.0221 m^2 for the car's frontal area ($A_{frontal}$) was calculated by applying the frontal car view on a grid of unit area and then counting the amount of squares contained with the car of given vehicle width and height. The actual C_D data is produced under real parameters, much of which we considered insignificant during current tests. Ideal conditions were assumed and a few factors were negligible. The car was then tested in a virtual wind tunnel by applying all real world principles and including all external car parts. Figure 2 shows the model under tests while the Table 2 shows force readings at a speed of about 17 m sec^{-1} (55 feet sec^{-1}).

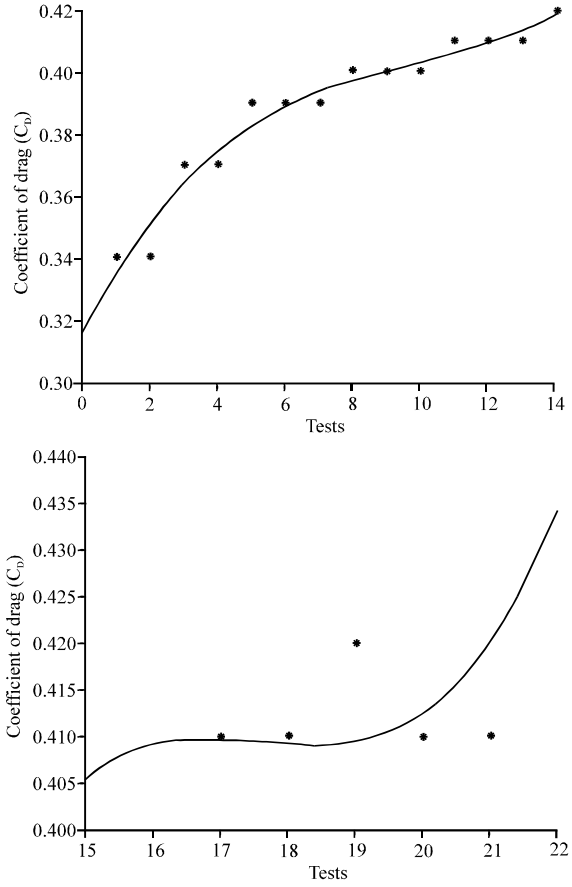

Fig. 2: Drag coefficients vs. tests (average drag coefficient, C_D is 0.40)

Using Eq. 1, we can find the drag coefficient of the car which is in essence traveling at 55 f sec^{-1} (or 16.76 m sec^{-1}) and experiencing 353.61 lbf (1572.92 N) of drag forces, with a frontal area $A_{frontal}$ of 22.10 m^2 (since the car is 10 times the model, area is 100 times the model) and ρ_{air} of 1.184 kg m^{-3} or C_D is 0.428. Compared to the real wind tunnel test data of 0.40, the virtual simulation yields a 7% increase in the Coefficient of Drag (C_D). This supports the earlier assumption relating to turbulent flow at the wheels and vehicle undercarriage. Since the virtual wind tunnel takes into account an uneven undercarriage and irregular contours at the wheels. On another note, there is a 2.73% decrease from the literature data of full scale real wind tunnel C_D of a car of the same model which is attributed towards the failure of the computation tool to take all real world parameters into consideration during fluid flow analysis and solving governing flow equations (Navier-Stokes equations), such as modeling relative to turbulence (Acheson, 1990). Most wind tunnel flows are usually simulated with the Navier Stokes Equation (Obayashi *et al*., 1998). Turbulence is a time dependent chaotic behavior seen often in many fluid flows (including air flows) caused due to the inertia of the fluid as a whole to the culmination of time dependent acceleration; or flows where inertial behavior is insignificant and laminar. It is generally believed that the Navier-Stokes equations describe turbulence (Batchelor, 1967).

Table 1: Wind tunnel data

Total height H (cm)	Height change ρh (m)	Drag force F_D (N)	Velocity u (mph)
8.00	0.01	0.80	29.79
8.70	0.02	1.20	36.96
9.70	0.03	2.00	45.26
10.50	0.04	2.49	50.94
11.30	0.05	3.20	56.05
12.00	0.05	3.65	60.16
12.70	0.06	4.14	64.01
13.50	0.07	4.80	68.14
14.10	0.07	5.34	71.09
14.70	0.08	5.74	73.91
15.20	0.09	6.23	76.19
15.70	0.09	6.58	78.39
16.50	0.10	7.16	81.80
16.70	0.10	7.43	82.64
16.10	0.09	6.94	80.12
15.70	0.09	6.45	78.39
14.50	0.08	5.74	72.98
13.30	0.07	4.85	67.13
12.10	0.05	4.00	60.72
10.80	0.04	2.98	52.91
9.60	0.03	2.14	44.50
8.40	0.02	1.33	34.07

Table 2: Computation Fluid Dynamic model test results at 55 mph for overall vehicle body

Goal name	Value	Averaged value	Minimum value	Maximum value
V_{max} ft sec^{-1}	0	0	0	0
V_{mean} ft sec^{-1}	55	55	55	55
V_{max} ft sec^{-1}	110	110	110	110
Force l bf	353.61	353.61	353.61	353.61
F_X l bf	252.98	247.97	242.98	252.98
F_Y l bf	-114.68	-110.74	-105.74	-115.74
F_Z l bf	215.29	212.06	208.12	216.00

The numerical solution of the Navier–Stokes equations for turbulent flow is very complex and due to the significantly different mixing-length scales involved in the turbulent flow, the solution of this model requires such an extremely fine mesh resolution in which the computational time becomes significantly unrealistic (Orszag, 1970). Solutions to turbulent flow using a laminar solving technique usually result in a time-unsteady figure which does not converge appropriately. However, certain models such as the Reynolds-Averaged Navier Stokes Equations (RANS) in addition to utilizing turbulence models can be used in to maintain a level of accuracy in Computational programs. In addition, Large Eddy Simulation (LES) and Detached Eddy Simulation (DES) can numerically solve for the correct data at varying Reynold's Number (Benazza *et al*., 2007), however, it has economic limitation as it is an expensive computation tool and is financially not viable for virtual model testing. LES techniques, although meticulous and expensive than the RANS model has the ability to yield better results, since in it, larger turbulent scales are appropriately resolved (Yokokawa *et al*., 2002).

CONCLUSION

A reduction of drag forces significantly helps the cars efficiency. Corrected design changes with verifiably lower coefficient of drag simply means that more energy will be going to the wheels of the car, as opposed to being used up in counteracting the drag forces that is exerted on the body by the air during motion. This translates to more miles per unit volume of fuel which in turn can mean lesser emissions given off by the car to travel the same distance. In most cases, the costs required to lower the drag coefficient pales in comparison to the fuel costs the car saves by being aerodynamically sound. Certain common automotive designs save money on the fuel and provide more force to the drive train, meaning valuable supplied force will not be wasted on overcoming air friction and drag forces.

ACKNOWLEDGMENT

This work would not have been possible without the guidance from Dr. Depcik at the University of Kansas and the help of Jason Carter and all the students from the KU Ecohawks group, especially Lou McKown. I humbly acknowledge their support in this work.

This study by the Sustainable Automotive Energy Infrastructure (KANSAS ECOHAWKS Project) Initiative at the University of Kansas as funded by the Kansas Transporation Research Institute and was conducted at the Facilities of the Department of Aerospace Engineering, Lawrence KS.

REFERENCES

Abdul Bari, H.A., K. Letchmanan and R.M. Yunus, 2011. Drag reduction characteristics using aloe vera natural mucilage: An experimental study. J. Applied Sci., 11: 1039-1043.

Acheson, D.J., 1990. Elementary Fluid Dynamics. Oxford University Press, Oxford, UK.

Aird, F., 2000. Automotive Math Handbook. 1st Edn., MotorBooks International, Osceola, WI., USA.

Batchelor, G.K., 1967. An Introduction to Fluid Dynamics. Cambridge University Press, Cambridge, ISBN-10: 0521663962.

Benazza, A., E. Blanco and M. Abidat, 2007. 2D detached-eddy simulation around elliptic airfoil at high reynolds number. J. Applied Sci., 7: 547-552.

Bernoulli, D., J. Bernoulli and J. Bernoulli, 2004. Hydrodynamics and Hydraulics. Dover Publications, New York.

Buckingham, E., 1914. On physically similar systems: Illustrations of the use of dimensional equations. Phys. Rev., 4: 345-376.

Chen, J., X. Fan and H. Hu, 2004. Numerical simulation of the external flow around a car body. J. Chongqing Univ., CNKI:SUN:FIVE.0.2004-10-033

Feynman, R.P., R.B. Leighton and M. Sands, 1963. The Feynman Lectures on Physics. Vol. 1, Addison-Wesley, New York, USA., ISBN-13: 9780201021165, pp: 14.

Liu, Y., 2006. Aerodynamic performance of off-design highly laded blade: A case study. J. Applied Sci., 6: 767-774.

Obayashi, S., K. Fujii and S. Gavali, 1998. Navier-stokes simulation of wind-tunnel flow using LU-ADI factorization algorithm. National Aeronautics and Space Administration (NASA), Ames Research Center. http://catalogue.nla.gov.au/Record/4022282.

Oertel, H., L. Prandtl, M. Bohle and K. Mayes, 2004. Prandtl's Essentials of Fluid Mechanics. Springer, Berlin, pp: 70-71.

Orszag, S.A., 1970. Analytical theories of turbulence. J. Fluid Mech., 41: 363-386.

Shirani, E., 2001. Compressible flow around a circular cylinder. J. Applied Sci., 1: 472-476.

Tipler, P.A., 1991. Physics for Scientists and Engineers. 3rd Edn., Worth Publishers, New York, USA., ISBN-13: 9780879014322, pp: 1517.

Ul Islam, S. and C.Y. Zhou, 2009. Numerical simulation of flow around a row of circular cylinders using the lattice boltzmann method. Inform. Technol. J., 8: 513-520.

Wang, M., Z. Liu and S. Huang, 2005. The application of FLUENT software in the car styling. Machinery Design Manufacture,

Yokokawa, M., K. Itakura, A. Uno, T. Ishihara and Y. Kaneda, 2002. 16.4-Tflops direct numerical simulation of turbulence by a fourier spectral method on the earth simulator. Proceedings of the 2002 ACM/IEEE Conference on Supercomputing, Nov. 16-22, Baltimore, MD., pp: 1-17.

Zhang, W., S. Hu, X. Song and Y. Bi, 2007. Numerical simulation and study of aerodynamic drag coefficient of automobile. Tractor Farm Transporter,

Zheng, C., S. Hu and K. Chen, 2001. Numerical analysis of the flow-field around 3-D car body using CFD. J. Univ. Shanghai For. Sci. Technol.